X-646-72-370

PREPRINT

NASA TM X- 66063

ELECTRON PRECIPITATION PATTERNS AND SUBSTORM MORPHOLOGY

R. A. HOFFMAN

J. L. BURCH

OCTOBER 1972

GSFC — GODDARD SPACE FLIGHT CENTER —

GREENBELT, MARYLAND

(NASA-TM-X-66063) ELECTRON PRECIPITATION PATTERN AND SUBSTORM MORPHOLOGY R.A. Hoffman, et al (NASA) Oct. 1972 49 p CSCL 04A

N73-10393

Unclas

G3/13 45698

ELECTRON PRECIPITATION PATTERNS AND SUBSTORM MORPHOLOGY

R. A. Hoffman

J. L. Burch

NASA-Goddard Space Flight Center
Greenbelt, Maryland 20771

OCTOBER 1972

ABSTRACT

Patterns of the precipitation of low-energy electrons observed by polar satellites have been examined as functions of substorm phase. Precipitation boundaries are generally identifiable at the low-latitude edge of polar cusp electron precipitation and at the poleward edge of precipitation in the pre-midnight sector (18-23 hrs. MLT). Both of these boundaries move equatorward when the interplanetary magnetic field (IMF) turns southward. Intense spikes of 2.3 kev electrons occurred in all quiet (IMF south) or growth phase cases in the pre-midnight region. The pre-midnight precipitation boundary remains at the same latitude on the average throughout the growth and expansion phases. However, during the expansion phase localized bands of intense 7.3 kev electrons are observed in the pre-midnight sector. Near and just after midnight intense 7.3 kev precipitation occurs over $\sim 10^{o}$ of latitude with a clear separation between lower latitude diffuse and higher latitude structured precipitation. During the recovery phase the diffuse band of energetic electrons, which first appeared near midnight, drifts through the morning hours to near noon, producing the mantle aurora. The high-latitude boundary of these drifting electrons occurs at higher latitudes for northward IMF and at lower latitudes for southward IMF. During the post-recovery phase, with northward IMF, the polar cusp and pre-midnight precipitation boundaries are again found at their quiet phase locations, but the diffuse band of drifting high-energy electrons continues to precipitate with the mantle aurora excitation continuing throughout the several hours required for the electrons to drift from midnight to noon.

The high-latitude precipitation boundary at 18-23 hrs. MLT is much sharper in the growth and expansion phases than can be explained by any observed plasma sheet gradients. It is concluded that a sharp boundary to closed field lines exists in the tail, perhaps as an X-type neutral line, throughout the growth and expansion phases. The statistical stability of the high-latitude precipitation boundary indicates that the postulated X-type neutral line is stationary in terms of the total flux of closed magnetic field lines which it defines.

INTRODUCTION

Early studies of magnetospheric substorms were necessarily confined to the polar magnetic substorm and the auroral substorm, which could conveniently be observed with ground-based instruments. One might expect, then, that experiments aboard low-altitude satellites and sounding rockets would provide data most pertinent to understanding these phenomena originally defined from ground-based measurements, and which have been related for decades to the bombardment of the upper atmosphere by charged particles.

Yet, one finds that the recent significant advances in our concepts of substorm morphology on a magnetospheric scale have come predominantly from experiments aboard satellites at large distances from the earth, and that the majority of the pertinent experiments have measured magnetic fields rather than particles (Fairfield and Ness, 1970; Aubry et al., 1970; Lezniak and Winckler, 1970; Aubry and McPherron, 1971; Hones et al.,1971).

Upon further investigation, one finds two principal reasons for this course of development. First, the low-altitude substorm phenomena are manifestations of a magnetospheric phenomenon (Coroniti et al., 1968) with important observables at large distances. Second, the analysis procedures for data derived from particle experiments from low-altitude satellites have fallen predominantly into two categories: either individual example passes are displayed to illustrate some particular feature of the precipitation profile (Burch, 1968; Hoffman, 1969; Heikkila and Winningham, 1971; Frank and Ackerson, 1971) or else rather gross statistical analyses or averages of features are presented (Sharp and Johnson, 1968; Craven, 1970; Hoffman and Berko, 1971). In neither case does the analysis pertain directly to substorm morphology.

This course of events is primarily due to the limitations of particle data obtained from low-altitude satellites. From a single satellite pass during a substorm only a few-minute snapshot pertaining to the particle precipitation pattern as a function of latitude at a particular local time is obtained under uncontrolled and often unknown conditions. Substorm development is rapid in comparison to a sequence of passes at the same local time, so that the temporal development of a single substorm cannot be followed. Finally, space-time variables cannot be separated. Statistical analysis of the data can serve to separate gross spatial features from some temporal effects. However, past statistical analyses have concentrated on the spatial features and have mainly ignored the temporal development of these features, at least on a scale applicable to substorm temporal development.

In this paper we have attempted an analysis of data primarily from the Auroral Particles Experiment aboard the OGO-4 satellite (Hoffman and Evans, 1968) in a statistical framework interpretable in terms of magnetospheric substorm morphology, both spatial and temporal.

SUBSTORM MODEL

To associate particle data directly with substorm morphology, it is first necessary to define the key features of a substorm to which the data will be associated. We divide a substorm into five phases and define these phases in terms of the interplanetary magnetic field latitude or Z component (in solar magnetospheric coordinates), auroral zone and polar cap magnetic activity, and the configuration of auroral forms. In Table 1 a summary of the criteria we have used in classifying the OGO-4 data is

given. Because heavy reliance was placed on the implications of auroral zone magnetograms, only those UT periods were used when fairly good local time coverage was available around midnight. DP2 signatures in polar cap and equatorial magnetograms were used in conjunction with interplanetary magnetic field data in determining the time of arrival of southward field at the earth to distinguish the quiet and growth phases. All-sky camera data were used only in confirming the distinction between growth phase and expansion phase.

Although the expansion phase can be recognized from magnetograms alone, there is now quite convincing evidence that it will not commence until the interplanetary magnetic field remains southward for over an hour (Arnoldy, 1971; Foster et al, 1971), although storm sudden commencements often induce premature expansion phase onsets (Burch, 1972a). We have added a post-recovery phase, in which the conditions cited are identical to the quiet phase, but which we will show is distinguishable by the particle precipitation data.

In the context of this model we will consider primarily electron precipitation information with the following spatial separation; first on the dayside at high latitudes, then in the pre-midnight sector, thirdly at post-midnight hours, and finally through the morning hours to noon.

DAYSIDE

It is now generally accepted that magnetosheath particles penetrate into the magnetosphere on the dayside and can be observed at low altitudes (Heikkila and Winningham, 1971; Frank, 1971). Quite a number of low-altitude dayside phenomena are apparently associated with these particles (see Hoffman, 1972, for a summary). Since the lowest energy detector in the Auroral Particles Experiment measured electrons in the high-energy

tail of the cusp region electrons (or dayside soft zone) the location of this region as a function of substorm phases could be studied. It was previously shown that the latitude of this precipitation grossly depends upon magnetic activity (Hoffman, 1972). However, Burch (1972b) has reported a systematic movement of the latitude of polar cusp precipitation during the early stages of substorms. These results are summarized here for completeness.

We interpret the low-latitude boundary of the cusp region electrons as the last closed field line on the dayside (see Burch, 1972b, Figure 1 for an example). Any large change in latitude of this field line can be attributed only to a change in the magnetospheric configuration, specifically the number of closed field lines in the dayside magnetosphere. It is not possible to lower the latitude of this precipitation by compressing the magnetosphere. Burch (1972b) showed that the tilt angle dependence of the latitude of this last closed field line was only 4^{o} for both seasonal and diurnal variations, and that during the quiet phase the average latitude was $\sim 77^{o}$.

However, he found that much larger changes in the location of the lower latitude boundary occurred as a function of time into the growth phase, or time after the interplanetary magnetic field turned southward (Figure 1). Since the only known cause for this variation is a decrease in the number of closed field lines in the dayside magnetosphere, this analysis provides a measurement on the rate of erosion of field lines on the dayside. This rate is 1^{o} every ten minutes during an average value for the southward interplanetary magnetic field of 3γ. Because it has

been observed that the magnetic field intensity in the tail region away from the plasma sheet increases during this phase, it is concluded that these dayside field lines are swept back by the solar wind into the tail (Fairfield and Ness, 1970).

This is the basic contribution to substorm morphology of the dayside cusp region. During the expansion phase the region remains at the lower latitude and returns to the quiet conditions during the recovery phase of a temporally isolated substorm. This behavior has also been inferred from observations of dayside auroras by Akasofu (1972) and in one case from the measurement of the inward motion of the magnetopause prior to the onset of a substorm expansion phase by Aubry et al., (1970).

PRE-MIDNIGHT

The behavior of particle precipitation patterns on the nightside is much more complex. To date only during the period 18-23 hrs. MLT have we been able to ascertain clearly the characteristics of precipitation patterns for all phases of the substorm. In Figures 2 and 3 are shown data from four passes of OGO-4 in this local time interval during the quiet, growth, expansion and recovery phases.

In Figure 2, auroral zone magnetograms for the midnight sector indicate that quiet conditions existed before and during Orbits 2958 and 3312. Data from the Ames magnetic field experiment on Explorer 33 are shown for the period prior to and just after Orbit 2958. Due to an error mode which occurred during this period, precluding measurement of the longitude of the interplanetary magnetic field (IMF), it was not possible to transform the vector magnetic field measurements from solar-equatorial (GSEQ) to

solar-magnetospheric (GSM) coordinates. However, by assuming a worst case IMF longitude and transforming the resulting vector, it is shown that the IMF was GSM northward for more than two hours prior to Orbit 2958. Electron fluxes for this pass were typical for these conditions; that is, very low energy electron precipitation persisted to high latitudes (on the average, about 79^{o}) and there was no significant precipitation of electrons at 7.3 kev (a typical energy for visual auroras).

Although the nightside auroral zone was also magnetically quiet during Orbit 3312 (shown in the right-hand panel of Figure 2), there was a significant difference in the latitude of the IMF for the previous hour and in the electron precipitation pattern. Data from Explorers 33 and 35 show that the IMF turned southward near 0720 UT, became horizontal near 0800, and again turned southward approximately 10 minutes before the 0830 high-latitude pass of Orbit 3312. A slight negative X deviation was apparent at Churchill at 0830 and the onset of the expansion phase is evident in the College and Churchill traces approximately 20-25 minutes later. The poleward boundary of electron precipitation is found at much lower latitudes during such conditions, here about $73\text{-}74^{o}$. Again, no significant 7.3-kev electron precipitation was present. There were, however, significant fluxes of 2.3 kev electrons which occurred in a band near the low-latitude edge of 0.7 kev precipitation and in a very intense spike in the higher-latitude region of 0.7 kev fluxes. This behavior has been observed in all quiet (IMF south) cases. Previously, Frank and Ackerson (1971) also noted that narrow bands of intense precipitated electrons, which they termed inverted V's, occurred in the

evening MLT sector during periods of relative magnetic disturbance (Kp = 3 to 4+). Examination of magnetograms and IMF data has indicated that several of the cases reported by Frank and Ackerson occurred during quiet (IMF south) or growth phase conditions. The energy flux contained in the high-latitude 2.3 kev spike in Figure 2 is approximately 16 ergs/cm^2sec kev at 2.3 kev and 7 ergs/cm^2sec kev at 0.7 kev. This energy flux is sufficient to account for the quiet auroral arcs which are often observed in this MLT sector (see Ackerson and Frank, 1972).

The sharp contrast between quiet-time electron precipitation for northward IMF and that for southward IMF shown in Figure 2 is typical of all such cases encountered whether or not a subsequent substorm expansion phase occurred. We are thus led to equate quiet (IMF south) conditions with growth phase conditions and will hereinafter use these two designations interchangeably.

A typical example of the electron precipitation pattern during the expansion phase in the pre-midnight hours is shown in the left panel of Figure 3. As during the growth phase, a sharp poleward boundary of 0.7 kev precipitation is evident near $\Lambda = 70^{\circ}$. However, during the expansion phase localized regions of intense 7.3 kev electron fluxes are present, extending up to, but never beyond, the sharp boundary of 0.7 kev precipitation. Again, the substorm phase was deduced by examining all available nightside high-latitude magnetograms, thereby obtaining as complete a representation as possible of the development of the substorm in universal time, rather than in local time as seen by a single station. Note in the left-hand panel of Figure 3 that the Dixon and Chelyuskin traces show a

near-simultaneous negative bay onset at approximately 1820 UT which we interpret as the beginning of the expansion phase of the first of several substorms. Leirvogur and Kiruna, in evening hours, experienced positive bays initially and then rotated into the negative bay region. Although a large negative bay was in progress at Leirvogur just as OGO-4 passed nearly overhead, this has not been used as a requirement for an expansion phase designation. In the case of smaller substorms only weak positive activity is often present under the satellite track while, near midnight, a sharp negative bay onset has occurred. Such cases have also been designated as expansion phase.

The observation of Ackerson and Frank (1972) of spatial coincidence between an auroral arc and an inverted V structure in the evening MLT sector was made during a period meeting our criteria for the expansion phase. In Plate 2 of Ackerson and Frank a very sharp high-latitude boundary of precipitation is apparent at all energies, which is consistent with the behavior noted in Figure 3.

Also shown in the expansion phase example of Figure 3 are the latitude regions in which the ratio of the flux of 2.3 kev electrons at $\sim 0^{o}$ pitch angle to that at $\sim 60^{o}$ pitch angle exceeded 2, the value which Berko (1972) has used as the criterion for field-aligned electron bursts. As discussed below, field-aligned 2.3 kev electron bursts were found by Berko to be a typical feature of the expansion phase passes.

Typical behavior late in the recovery phase with a northward IMF is shown in the right-hand panel of Figure 3. The precipitation pattern in evening hours is much the same as during quiet (IMF north) conditions,

with 0.7 kev fluxes extending to near 80° and no significant influx of 7.3 kev electrons.

In the OGO-4 data, the most consistently observed characteristics of the high-latitude electron precipitation patterns in the evening sector (18-23 hours MLT) during the first four substorm phases which can be related to substorm morphology are:

(1) the systematic variation in latitude of the high-latitude boundary of 0.7 kev precipitation;

(2) the relative positions of the low-energy (0.7 kev) and high-energy (7.3 kev) electron boundaries, which often coincide during the expansion phase.

(3) the occurrence of significant fluxes of 7.3 kev electrons only during the expansion and early recovery phases.

A study of the complete set of 1-1/2 years of OGO-4 data in conjunction with ground magnetograms, IMF measurements from Explorers 33 and 35, and the published data of Frank and Ackerson (1971) resulted in 61 cases when the substorm phase, IMF latitude and the 0.7 and 7.3 kev electron high-latitude boundaries could be determined unambiguously. The results are shown in Figure 4 for four phases of a substorm. All data points locate the high-latitude boundary of 0.7 kev electron precipitation. For this local-time sector a post-recovery phase is not distinguishable from the quiet phase in the electron data. The open points in Figure 4 are from OGO-4 data while the solid points were obtained from the published data of Frank and Ackerson (1971) and Ackerson and Frank (1972). It is evident from Figure 4 that:

(1) all quiet phase electron boundaries for northward or horizontal IMF were at $\Lambda > 75^{o}$;

(2) all quiet phase electron boundaries for southward IMF (i.e., growth phase) were at $\Lambda < 74^{o}$;

(3) the expansion phase electron boundaries were in the same latitude range as those during the growth phase; that is, the average of all boundary locations for early and maximum expansion were 71.3^{o} and 71.7^{o}, compared with the growth phase average of 71.5^{o};

(4) the precipitation boundary was again found at higher latitudes during the late recovery phase provided the IMF had turned northward. There were two such cases when the boundary remained at $\Lambda < 75^{o}$, but one of these was associated with large and rapid variations in the IMF direction.

We return now to the expansion phase behavior in pre-midnight hours and the apparent stability in the location of the precipitation boundary through the growth and expansion phases which was noted in (3) above. In Figure 5 we have plotted the difference in latitude of the 0.7-kev and 7.3-kev high-latitude boundaries for the expansion phase and 18-23 hrs. MLT. The two obvious features to note are:

(1) at no time does the 7.3-kev precipitation occur at higher latitudes than the 0.7-kev precipitation, and

(2) there is a tendency for the 7.3-kev precipitation boundary to lie at lower latitudes than the 0.7-kev boundary during the early expansion phase.

It appears that during the expansion phase the westward and northward surge brings the more energetic or visual auroral electron fluxes up to the 0.7 kev precipitation boundary. Furthermore, this boundary location for all precipitation with energy > 0.7 kev seems to have been pre-established during the substorm growth phase. However, this conclusion is based on the location of the boundaries during the growth and expansion phases averaged over a number of substorms, and cannot be verified by data from successive passes during a single substorm.

The behavior of the precipitation noted in (1) and (2) above suggests that the energetic expansion phase electron fluxes are produced by acceleration of a portion of the large reservoir of low-energy electrons which are already being precipitated, rather than by impulsive injection of new particles. Assuming that the origin of these high-latitude energetic electrons is the tail plasma sheet, an obvious question to ask is what stable feature exists in the tail both during the growth and expansion phases to limit the latitude of precipitation. This question will be considered further in the discussion section.

As previously mentioned in the discussion of the expansion phase example (Figure 3), a typical feature of this substorm phase is the appearance of field-aligned 2.3 kev electron bursts. Berko (1972) has studied the occurrence of such field-aligned events for the OGO-4 quiet, growth and expansion phase cases plotted in Figure 4. For completeness we repeat here his principal results:

(1) isolated field-aligned events were observed in five of the twelve quiet (IMF north) cases analyzed;

B

(2) no field-aligned events were observed in the six quiet (IMF south) or growth phase cases;

(3) field-aligned events were observed in all expansion phase cases, covering regions up to 4^{o} wide in latitude in some cases.

(4) These field-aligned events tended to occur in the high-latitude portion of the 0.7 kev precipitation region.

POST-MIDNIGHT AND MORNING HOURS

In contrast to the rather localized bands of 7.3 kev electrons observed in the pre-midnight region, the expansion phase precipitation near and just after midnight is intense and widespread, covering 10^{o} or more in latitude. This local-time difference in precipitation patterns between the pre-midnight region (where positive bays predominate) and the midnight and post-midnight region (where negative bays predominate) has previously been pointed out by Burch (1972c). Figure 6 provides an example of the expansion phase behavior near 3 hrs. MLT. As in the pre-midnight region, sharp, coincident high-latitude precipitation boundaries occurred for both 0.7 and 7.3 kev electrons. The most striking recurring feature of expansion and recovery phase precipitation in midnight and post-midnight hours is the separation between diffuse and structured precipitation, occurring in Figure 6 at $\Lambda \approx 69.5^{o}$.

Hoffman (1970) and Gustafsson (1972) have found evidence that the intense diffuse band of auroral electrons injected near midnight during the expansion phase drifts through the morning hours to or just beyond noon, producing the mantle aurora. Further evidence for this explanation is presented in Figure 7. During Orbit 6691, OGO-4 crossed the

auroral zone near 6.8 hours MLT about 15 minutes after the onset of a substorm expansion phase, which followed an extended period of magnetic quiet. In this pass, 0.7 kev electrons were observed from $\Lambda \simeq 73.5^{o}$ to 79^{o}, but no 7.3 kev precipitation was detected. In another example in the right-hand portion of Figure 7, the development of a drifting band of high-energy electrons, or hard zone, is clearly evident during the successive orbits 6736 and 6737. Near 1845 UT, approximately 50 minutes after the onset of the first of three negative bays at Chelyuskin, only weak precipitation of 7.3 kev electrons occurred near 7 hrs. MLT in the invariant latitude range 70.5^{o} to 75^{o}. No precipitation was noted at lower latitudes. In the next pass, near 2025 UT, or 2.5 hours after the onset of substorm activity, a broad band of 7.3 kev electron precipitation is apparent in the region $\Lambda \approx 66^{o}$ to 71^{o}, where in the previous pass no electrons were detected. Weaker, structured 7.3 kev precipitation was still present at higher latitudes as in Orbit 6736. Because of its location in latitude and structured appearance we identify this higher latitude 7.3 kev precipitation as the high-energy tail of soft zone precipitation and not as drifting substorm-injected electrons.

In contrast to the electron precipitation in the polar cusp and premidnight regions, which return to quiet condition patterns in the post-recovery phase, the diffuse band of energetic electrons continues to exist in the dawn and morning sector for several hours after a substorm. Two examples of such post-recovery precipitation at approximately 9-10 hours MLT are displayed in Figure 8. The electron data in Figure 8 were taken from Frank and Ackerson (1971). The data shown on the left were taken after the full recovery of substorm activity, while the pass on the right occurred during a period between substorms. The diffuse band of energetic electrons is evident in both cases, although its high-latitude boundary is located several degrees higher in latitude in the example on the left (when the IMF was northward) than in the example on the right (when the IMF was southward).

These examples clearly illustrate the dynamic nature of the various precipitation regions and the need for specification of substorm phase and IMF direction before any meaningful predictions of their locations and extent can be made.

The statistical location of diffuse 7.3 kev electron precipitation is shown in Figure 9. This drifting band of precipitation begins to appear at about 19 hrs. MLT, where it occurs in localized narrow bands or inverted V's. It extends through the morning hours to noon, at increasing latitudes, where it produces the sub-visual mantle aurora. An estimate of the total energy contained in this diffuse precipitation is 3×10^{17} ergs/sec over a period of several hours, or a total single substorm energy input of about 10^{21} ergs. Because the auroras that this precipitation produces are sub-visual, this energy input, which is comparable to that producing visual auroras, is usually ignored in discussions of substorm energetics.

SUMMARY

The results of this study are summarized in Figure 10 with five illustrations, one for each phase of the substorm. (1) During the quiet period, the dayside cusp region lower boundary lies at about 77^{o}, and the pre-midnight high-latitude boundary for all precipitation of > 0.7 kev electrons lies at about 79^{o}. There is no hard zone in the dawn and late morning hours if no substorm has occurred in the previous few hours. (2) The onset of the reconfiguration of the magnetosphere commences when the IMF turns southward. The dayside particle data provide excellent evidence for the subsequent erosion of dayside magnetic flux. The poleward boundary for 0.7 kev electron precipitation on the nightside also

moves to considerably lower latitudes, although whether this is a sudden or gradual change has not been measured. (3) During the expansion phase in pre-midnight hours, localized 7.3 kev precipitation is observed to move up to, but never beyond, the 0.7 kev poleward boundary which was established during the growth phase. Near and just after midnight, intense and widespread 7.3 kev precipitation is observed over $\sim 10^{o}$ of latitude up to a sharp poleward boundary which coincides with the 0.7 kev boundary. A separation between diffuse and structured precipitation is often apparent in this region, with at least the diffuse band of precipitation apparently occurring on closed field lines. (4) During the late recovery phase, provided the IMF has turned northward, the dayside cusp is again observed at $\sim 77^{o}$, the poleward boundary of > 0.7 kev precipitation in pre-midnight hours is again found at latitudes as high as, or possibly higher than during the quiet period, and the diffuse band of high-energy electrons which appeared on closed field lines near midnight begins to drift through the morning hours. (5) We have added a post-recovery phase, during which magnetospheric conditions are the same as during the quiet period, except that the diffuse band of drifting high-energy electrons continues to precipitate into the ionosphere from early morning hours to near noon, producing the mantle aurora. The mantle aurora excitation continues throughout the $\sim$ 6 hr. period required for the 7 kev electrons to drift from midnight to noon.

DISCUSSION

We return now to a consideration of the lowering of the high-latitude precipitation boundary in pre-midnight hours and its apparent stability

through the growth and expansion phases. For the elongated magnetic tail configuration which exists during the growth phase, it is expected that the field lines passing near the high-latitude precipitation boundary ($\Lambda \simeq 70^{o}$) in the sector 18-23 hrs. MLT will extend into the region of the tail plasma sheet. It appears then, that some stable feature exists in the tail region during the growth and expansion phases to limit the latitude of precipitation. Two possible candidates are a sharp plasma density gradient or a boundary to closed field lines (lines threading across the plasma sheet).

We first consider density gradients in the tail. The literature contains very little information relating to the gradient of the plasma sheet in the $-X_{GSM}$ direction. Burke and Reasoner, (1971) report decreases of intensities by several orders of magnitude between 20 and 60 R_E coincident with auroral substorms or at the center of the tail at lunar distances during quiet times. Density gradients in the $-X_{GSM}$ direction should be reflected into gradients in the Z direction if we make the now common assumption that plasma boundaries are aligned along magnetic field lines. While no growth phase measurements of the thickness of the plasma boundary in the Z direction have been reported, Hones et al. (1971) have observed that (1) during quiet times the plasma sheet particle density falls off gradually over a ΔZ of about 2 R_E, and (2) during the substorm expansion phase, when the plasma sheet is expanding, the boundary is sharper, with the particle density gradient occurring over a ΔZ of only 2000 to 3000 km.

At high latitudes and low altitudes we can obtain a "boundary thickness" by observing the details of the cut-off of precipitation. In Figure

11 we have plotted on an expanded time scale the 0.7 kev electron fluxes across the high-latitude precipitation boundary for five of the six OGO-4 cases associated in Figure 4 with quiet (IMF south) or growth phase conditions. These boundaries are extremely sharp, with no indication of a gradual decrease in intensity. The sixth case exhibited a complicated boundary structure which extended over about a half degree in latitude. Whether this was temporal structure or an indication of a wide boundary region cannot be determined. Hence, we take the normal high-latitude boundary to be $\sim 0.05^{\circ}$ wide. We will also assume a ΔZ thickness of $\sim$ 2500 km during the growth phase on the basis of the similarity of the high-latitude precipitation boundaries during the growth and expansion phases reported herein as well as the observation of plasma sheet thinning during the growth phase made by Aubry and McPherron (1971). A ΔX thickness of several tens of R_E will be assumed based on the report of Burke and Reasoner (1971).

We next look for consistency in the three "measurements" of boundary thickness through conservation of magnetic flux through the respective boundaries:

$$\Phi \text{ (high-latitudes)} = \Phi\ (\Delta Z) = \Phi\ (\Delta X),$$

or

$$\int_{\phi_1}^{\phi_2}\int_{70^{\circ}-\Delta\Lambda}^{70^{\circ}} B(\text{earth}) \sin\Lambda \cos\Lambda\, d\Lambda d\phi = B(\text{tail})\ \Delta Y\ \Delta Z = B(\text{neutral sheet})\ \Delta Y\ \Delta X,$$

where we assume that the longitude interval $\phi_2 - \phi_1 = 15^{\circ}$ maps into a width $\Delta Y = 3R_E$ in the tail (see, for example, Fairfield and Ness, 1970),

and set B(earth) = 62,000γ, B(tail) = 20γ and B(neutral sheet) = $\frac{1}{2}\gamma$. For a $\Delta\Lambda$ of 0.05°, ΔZ should be 480 km, compared with a measured value of $\sim$ 2500 km, and ΔX = 3.0 R_E, considerably less than any reasonably expected gradient. However, for ΔZ = 2500 km, ΔX = 15.7 R_E, which is consistent with the observations. Therefore, while the tail measurements are consistent, the plasma properties do not reflect down to low altitudes.

However, it is of importance in this context that the boundary measured by OGO-4 is a precipitation boundary, and as such gives no information about particles mirroring above the satellite altitude of about 700 km. Therefore, any mapping of this boundary into a plasma sheet boundary at 18 R_E (the Vela distance) is predicated on the existence of an efficient precipitation mechanism on the field lines considered. Although the process by which plasma sheet electrons are precipitated is not completely understood, some possible mechanisms (Kennel and Petschek, 1966; Sharber and Heikkila, 1972) require that the field lines must be closed in the sense that they must cross the neutral sheet.

We next consider an X-type neutral line as a possible boundary to closed field lines in the $-X_{GSM}$ direction. This growth phase neutral line would produce a sharp high-latitude precipitation boundary more in keeping with the observations in Figure 11. On the basis of the apparent stability of this boundary through the growth and expansion phases it would define the total flux of closed magnetic field lines and the total particle population active in an entire substorm. It follows that all substorm associated precipitation would occur on closed field lines. Although a growth phase X-type neutral line has not been directly observed in the tail

region, such a configuration does provide a qualitative explanation for the sharp precipitation boundary observed at low altitudes.

The conclusions of this study are illustrated in the diagrams of the quiet, growth and expansion phase magnetospheres in Figure 12, drawn for the noon and pre-midnight magnetosphere.

In the quiet phase the tail field is somewhat dipolar with field lines originating at latitudes as high as 79° crossing the plasma sheet relatively near the earth. Higher latitude field lines map into the high-latitude tail where plasma densities are very low and eventually cross the plasma sheet at very large distances where plasma densities are also very low (Burke and Reasoner, 1971). It is possible that an X-type neutral point exists at a very large distance down the tail (> 60 R_E) during the quiet phase (Russell, 1972), serving to define the boundary between open and closed field lines which would determine the low-altitude precipitation boundary. During the quiet phase the IMF is northward and the magnetosphere is closed, with only a small amount of reconnection occurring across the magnetopause (Forbes and Speiser, 1971; Alfvén and Falthammer, 1971), and the dayside cusp lower boundary is located at about 77°.

In the growth phase, efficient dayside reconnection of southward IMF and magnetospheric field lines occurs, dayside magnetic flux is carried into the nightside magnetosphere, which is stretched into an elongated tail-like configuration, and the magnetosphere becomes open. It is observed that the plasma sheet thins during this time (Aubry and McPherron, 1971), but it is not compressed (Hones et al, 1971). Instead, plasma seems to escape from the upper and lower portions of the plasma sheet which was $\sim$ 6 R_E thick at 18 R_E during the quiet phase until it becomes only $\sim$ 2 R_E thick.

Our observation that the precipitation boundary moves to lower latitudes during the growth phase is explained by the establishment of an X-type neutral line at a lesser distance magnetically than the quiet phase neutral line (if one existed). The actual physical distance cannot be calculated by field line tracing from low altitudes or flux conservation considerations using presently available magnetospheric models. The growth phase X-type neutral line serves the dual purpose of a reconnection mechanism for tail field lines (which is required for convection of eroded dayside magnetic flux back to the day side) and a sharp boundary between closed field lines and open field lines, which are connected to some degree to the IMF. Plasma in regions of the quiet-phase plasma sheet lying at higher latitudes than the field line passing through the growth-phase X-type neutral line could then flow outward, escaping from the tail in the anti-solar direction. Loss of these particles through precipitation is less likely since they would be on open field lines and in a region of weak magnetic field.

Under the influence of the increased cross-tail electric field, particles on closed field lines would experience an $\bar{E} \times \bar{B}$ drift in the directions indicated by the arrows in Figure 12. Above and below the neutral sheet, where $B \sim B_X$, such a drift would carry the particles toward the neutral sheet. Near the neutral sheet, where $B \sim B_Z$, the $\bar{E} \times \bar{B}$ drift would be toward the earth, producing the earthward movement of the inner edge of the plasma sheet first observed by Vasyliunas (1968). We stress here that, whereas it is known that X-type neutral points exist in the tail (Schindler and Ness, 1972) and that they appear in conjunction

with the expansion phase onset (Camidge and Rostoker, 1970) no further studies of their existence as a function of substorm phase have been reported.

During the expansion phase, the pressure distending the tail is released beginning at near distances (lower diagram) by precipitation into the atmosphere. The release of pressure allows field lines to collapse to a more dipolar shape and accelerates particles by Fermi and betatron acceleration (Northrop, 1963). The pressure release region would travel to larger distances, perhaps in the manner proposed by Coroniti and Kennel (1972) until plasma on all field lines closing within the neutral line has been affected. This outward motion of pressure release by precipitation would produce the northward surge which would be bounded in its poleward motion by the precipitation boundary pre-established in the growth phase by the X-type neutral line. Although our measurements contain no information about the physical motion of the postulated neutral line during the expansion phase, they do indicate that, on a statistical basis, the neutral line is stationary in terms of the total flux of closed magnetic field lines which it defines. However, from the magnetic measurements of Fairfield and Ness (1970) and Camidge and Rostoker (1970),it is more likely that the neutral line physically moves in (accompanied perhaps by the formation of other neutral lines) rather than out (as proposed by Russell, 1972), since an outward movement would tend to decrease rather than increase B_Z in the tail.

During this dynamic phase, local potentials could build up, producing field-aligned currents as observed by the OGO-4 Auroral Particles Experiment and many other experiments (Berko, 1972). Strong pitch-angle scattering

and the multiplicity of processes would make difficult the unique indentification of acceleration mechanisms through particle observations alone. Field lines which have already relaxed would contain energized particles which would continue to precipitate in a more uniform manner by pitch angle scattering to produce the more diffuse auroras at latitudes below the active region (Figure 6). The electrons trapped on these field lines would begin a magnetic drift to the morning hours, eventually producing the mantle aurora.

Considerably more analysis is required to determine magnetospheric topology on the basis of data acquired by low-altitude polar satellites. Consideration must be given to the possibility that different regions of the tail can be simultaneously in different substorm phases. Such a consideration is crucial for understanding the magnetospheric topology and dynamics of multiple substorms.

TABLE CAPTIONS

TABLE 1. List of interplanetary and ground-based data used in the determination of substorm phase. The designation N/A indicates only that the particular type of data was not used in the phase determination, not that systematic variations do not occur.

TABLE 2. List of 0.7 kev precipitation boundary locations used in Figure 4. *'s indicate data from INJUN 5 (Frank and Ackerson, 1971 and Ackerson and Frank, 1972). +'s indicate growth phase cases which were verified with all-sky photographs taken at Great Whale River and Churchill. Other growth phase cases occurred on cloudy nights or at times when midnight photographs were not available.

SUBSTORM MODEL

PHASE	MIDNIGHT MAGNETOGRAM H TRACE	IMF	POLAR CAP AND EQUATORIAL MAGNETOGRAMS	MIDNIGHT ALL-SKY PHOTOGRAPHS
Quiet	Undisturbed	Northward	Undisturbed	N/A
Growth or Quiet (IMF South)	Gradual Negative Deviation or Undisturbed	Southward	Disturbed in Correlation with Southward-Turning IMF	No Breakup
Expansion	Sharp-Onset Negative Bay	N/A	N/A	Breakup and Poleward Expansion
Recovery	Recovering Toward Baseline	Northward	N/A	N/A
Post-Recovery	Undisturbed	Northward	N/A	N/A

TABLE 1

TABLE 2

DATA USED IN FIGURE 4

QUIET NORTH			
Date	U.T.	Λ	MLT
8/24/67	17.11	78.8	22.3
11/11/67	16.80	79.9	22.4
11/27/67	17.15	80.7	21.7
12/17/67	17.51	82.6	20.6
2/1/68	08.76	75.6	22.6
2/14/68	09.07	80.5	20.1
4/16/68	17.66	78.7	22.8
7/5/68	17.58	77.9	22.6
7/18/68	20.20	81.4	23.0
7/19/68	18.90	78.6	22.2
8/5/68	07.25	77.1	20.5
8/8/68	18.89	82.0	20.4
8/12/68	18.55	82.3	20.0
11/24/68	23.44	78.2	19.5
*12/2/68	02.05	76.0	22.2
1/4/69	16.50	78.0	19.8
QUIET SOUTH			
+ 2/6/68	09.12	71.0	22.2
3/9/68	08.50	73.4	18.9
10/25/68	08.61	69.5	20.8
11/12/68	21.78	71.8	22.6
11/14/68	20.71	69.9	22.5
11/19/68	20.48	72.1	22.3
+*12/2/68	04.09	70.3	21.8

QUIET SOUTH (CONT'D)			
Date	U.T.	Λ	MLT
*12/10/68	03.45	72.1	20.5
*12/16/68	04.46	73.3	19.2
EXPANSION			
10/2/67	09.04	70.2	21.6
10/14/67	07.86	74.0	19.8
10/17/67	07.55	75.6	19.1
10/24/67	07.39	72.3	19.1
10/24/67	09.00	72.7	19.2
11/5/67	10.97	73.0	19.2
2/16/68	09.83	73.4	21.0
3/3/68	07.85	72.7	19.3
3/4/68	08.22	69.9	19.5
3/4/68	22.82	68.8	22.9
3/10/68	21.84	69.8	22.8
3/27/68	20.10	76.0	23.0
4/5/68	20.10	69.9	20.0
6/1/68	09.56	72.3	20.6
6/27/68	11.73	74.5	18.9
10/2/68	09.99	75.1	22.3
10/5/68	09.23	70.6	22.5
11/8/68	09.37	71.8	18.0
11/17/68	18.30	66.7	21.9
11/17/68	21.53	70.1	21.6

EXPANSION (CONT'D)			
Date	U.T.	Λ	MLT
11/24/68	18.60	68.7	21.5
11/26/68	17.55	70.2	21.5
12/3/68	03.74	73.4	21.5
12/8/68	06.21	72.2	21.2
12/11/68	18.30	71.6	20.0
*12/21/68	23.55	72.4	20.1
*12/21/68	01.87	70.4	19.4
RECOVERY			
8/15/67	17.77	77.7	22.3
1/22/68	11.3	> 85	22.8
2/16/68	08.18	71.5	21.1
2/25/68	08.42	71.7	20.1
3/6/68	09.00	74.3	19.2
4/27/68	10.29	82.2	20.1
10/11/68	09.39	73.4	21.7
11/13/68	22.06	74.0	22.8
12/1/68	20.50	76.4	21.5

REFERENCES

Ackerson, K. L., and L. A. Frank, Correlated satellite measurements of low-energy electron precipitation and ground-based observations of a visible auroral arc, J. Geophys. Res., 77, 1128, 1972.

Akasofu, S.-I., Midday auroras at the south pole during magnetospheric substorms, J. Geophys. Res., 77, 2303, 1972.

Alfvén, H., and C.-G. Fälthammar, A new approach to the theory of the magnetosphere, Cosmic Electrodynamics, 2, 78, 1971.

Arnoldy, R. L., Signature in the interplanetary medium for substorms, J. Geophys. Res., 76, 5189, 1971.

Aubry, M. P., and R. L. McPherron, Magnetotail changes in relation to the solar wind magnetic field and magnetospheric substorms, J. Geophys. Res., 76, 4381, 1971.

Aubry, M. P., C. T. Russell, and M. G. Kivelson, On inward motion of the magnetopause preceding a substorm, J. Geophys. Res., 75, 7018, 1970.

Berko, F. W., Distributions and charactersitics of high-latitude field-aligned electron precipitation, submitted to J. Geophys. Res., 1972.

Burch, J. L., Low-energy electron fluxes at latitudes above the auroral zone, J. Geophys. Res., 73, 3585, 1968.

Burch, J. L., Preconditions for the triggering of polar magnetic substorms by storm sudden commencements, J. Geophys. Res., 77, 5629, 1972a.

Burch, J. L., Precipitation of low-energy electrons at high latitudes: Effects of interplanetary magnetic field and dipole tilt angle, J. Geophys. Res., 77, , 1972b.

Burch, J. L., Effects of interplanetary magnetic sector structure on auroral zone and polar cap magnetic activity, submitted to J. Geophys. Res., 1972c.

Burke, W. J., and D. L. Reasoner, Absence of the plasma sheet at lunar distance during quiet times, EOS, Trans. AGU, 52, 906, 1971.

Camidge, F. P., and G. Rostoker, Magnetic field perturbations in the magnetotail associated with polar magnetic substorm, Can. J. Phys., 48, 2002, 1970.

Coroniti, F. V., and C. F. Kennel, Magnetospheric substorms, Cosmic Plasma Physics, ed. by K. Schindler, Plenum Press, New York, 15, 1972.

Coroniti, F. V., R. L. McPherron and G. K. Parks, Studies of the magnetospheric substorm, 3, concept of the magnetospheric substorm and its relation to electron precipitation and micropulsations, J. Geophys. Res., 73, 1715, 1968.

Craven, J. D., A survey of low-energy ($E \gtrsim 5$ kev) electron energy fluxes over the northern auroral regions with satellite Injun 4, J. Geophys. Res., 75, 2468, 1970.

Fairfield, D. H., and N. F. Ness, Configuration of the geomagnetic tail during substorms, J. Geophys. Res., 75, 7032, 1970.

Forbes, T. G., and T. W. Speiser, Mathematical models of the open magnetosphere: application to dayside auroras, J. Geophys. Res., 76, 7542, 1971.

Foster, J. C., D. H. Fairfield, K. W. Ogilvie, and T. J. Rosenberg, Relationship of interplanetary parameters and occurrence of magnetospheric substorms, J. Geophys. Res., 76, 6971, 1971.

Frank, L. A., Plasma in the earth's polar magnetosphere, J. Geophys. Res., 76, 5205, 1971.

Frank, L. A., and K. L. Ackerson, Observations of charged-particle precipitation into the auroral zone, J. Geophys. Res., 76, 3612, 1971.

Gustafsson, G., Latitude and local time dependence of precipitated low energy electrons at high latitudes, submitted to J. Geophys. Res., 1972.

Heikkila, W. J., and J. D. Winningham, Penetration of magnetosheath plasma to low altitudes through the dayside magnetospheric cusps, J. Geophys. Res., 76, 883, 1971.

Hoffman, R. A., Low-energy electron precipitation at high latitudes, J. Geophys. Res., 74, 2425, 1969.

Hoffman, R. A., Auroral electron drift and precipitation: cause of the mantle aurora, NASA-GSFC Preprint, X-646-70-205, June 1970.

Hoffman, R. A., Properties of low energy particle impacts in the polar domain in the dawn and dayside hours, Magnetosphere-Ionosphere Interactions, ed. by K. Folkestad, Universitetsforlaget, Oslo, p. 117, 1972.

Hoffman, R. A., and Berko, F. W., Primary electron influx to the dayside auroral oval, J. Geophys. Res., 76, 2967, 1971.

Hoffman, R. A., and D. S. Evans, Field aligned electron bursts at high latitudes observed by OGO-4, J. Geophys. Res., 73, 6201, 1968.

Hones, E. W., Jr., J. R. Asbridge and S. J. Bame, Time variations of the magnetotail plams sheet at 18 R_E determined from concurrent observations by a pair of Vela satellites, J. Geophys. Res., 76, 4402, 1971.

Kennel, C. F. and H. E. Petschek, Limit on stably trapped particle fluxes, J. Geophys. Res., 71, 1, 1966.

Figure 12: Possible magnetospheric configurations in the noon and pre-midnight meridians during quiet times and the growth and expansion phase of substorms based on the observed electron precipitation patterns and the assumption of a neutral line in the tail.

FIGURE CAPTIONS

Figure 1: Differences between the latitudes of observed lower boundaries of polar cusp electron precipitation and the expected boundaries (including tilt-angle effects) for 10 cases which followed sharp onsets of southward IMF (taken from Burch, 1972b). Listed alongside each point are (1) the average southward component of IMF during the period between the onset of southward field and the observation, and (2) for $\Delta\Lambda < 0$, the ratio of magnetic flux eroded into the tail to the southward magnetic flux brought to the magnetosphere as deduced from flux conservation calculations based on each $\Delta\Lambda$. The linear regression line represents an erosion rate of $\sim 0.1^{o}$/min.

Figure 2: Typical 0.7, 2.3 and 7.3 kev electron precipitation patterns during quiet times with IMF northward and southward. In these and all succeeding plots electron flux is in the units electrons/cm^2-ster-kev-sec. M's along the magnetogram traces indicate midnight MLT. Explorer 33 and 35 IMF data are from the Ames magnetometer experiment.

Figure 3: Typical 0.7 and 7.3 kev electron precipitation patterns during the expansion phase and late recovery phase (IMF north) of substorms for 18-23 hrs. MLT. Also shown in the expansion phase example are regions where the ratio of the flux of 2.3 kev electrons near 0^{o} pitch angle to that near 60^{o} pitch angle exceeded 2. These regions of field-aligned 2.3 kev electron bursts were identified in the study by Berko (1972).

Figure 4: A plot of the location of the high-latitude 0.7 kev electron precipitation boundary for 18-23 hrs. MLT. Open points were taken from OGO-4 data -- solid points from the data of Frank and Ackerson (1971) and Ackerson and Frank (1972). A list of the passes analyzed is given in Table 2. Substorm phase was deduced from all available magnetograms. Where possible the quiet (IMF south) cases were further confirmed by examining near-midnight all-sky camera pictures.

Figure 5: Plot of the difference between the latitude of the precipitation boundaries at 7.3 kev and 0.7 kev observed by OGO-4 during the expansion phase cases plotted in Figure 4. The 7.3 kev boundary is never found poleward of the 0.7 kev boundary and the two boundaries tend to coincide in the late expansion phase.

Figure 6: A typical example of 0.7 and 7.3 kev electron precipitation patterns during the expansion phase in post-midnight hours MLT. Note the clear separation between the lower latitude diffuse precipitation and higher latitude structured precipitation.

Figure 7: A set of OGO-4 passes showing the development of the diffuse band of drifting energetic electrons at $\sim$ 7 hrs. MLT following the substorm expansion phase.

Figure 8: Two examples of INJUN 5 electron data taken from Frank and Ackerson (1971), showing the existence of the diffuse band of drifting electrons at $\sim$ 9-10 hours MLT following substorms (dayside hard zone). In the example on the left the band

Figure 8: (Cont'd) extended up to $\Lambda = 78^{o}$ and terminated at an intense burst of low-energy electrons, which Frank and Ackerson identified as polar cusp electrons. The IMF was northward during this pass. In the example on the right, for a southward IMF, the high-latitude boundary between the drifting electrons and the adjacent polar cusp electrons was located at $\Lambda \sim 72.7^{o}$.

Figure 9: Average location in Λ and MLT of 7.3 kev electron precipitation observed on OGO-4 irrespective of magnetic activity. This data has been replotted from Figure 15 of Hoffman (1972). In pre-midnight hours the precipitation occurs in narrow bands. Near midnight, injection of intense fluxes occurs during the expansion phase, producing a diffuse band of electrons which drift through the morning hours to near noon.

Figure 10: Polar plots in Λ and MLT summarizing electron precipitation patterns for the five substorm phases.

Figure 11: Superposition of 0.29-sec. averages of 0.7 kev precipitated electron fluxes across the high-latitude boundary for five of the six OGO-4 quiet (IMF south) cases plotted in Figure 4. A complicated boundary structure occurred in the sixth case, indicating a possible moving boundary. Although spikes of precipitation are sometimes observed poleward of the boundary (as in Figure 2) they are generally 2 or more orders of magnitude less intense than the fluxes just equatorward of the boundary.

Lezniak, T. W., and J. R. Winckler, An experimental study of magnetospheric motion and the acceleration of energetic electrons during substorms, J. Geophys. Res., 75, 7075, 1970.

Northrop, T. G., The adiabatic motion of charged particles, Interscience Publishers, New York, 12, 1963.

Russell, C. T., The configuration of the magnetosphere, Publ. No. 1036, Univ. of California, Los Angeles, Calif., 1972.

Schindler, K., and N. F. Ness, Internal structure of the geomagnetic neutral sheet, J. Geophys. Res., 77, 91, 1972.

Sharber, J. R., and W. J. Heikkila, Fermi acceleration of auroral particles, J. Geophys. Res., 77, 3397, 1972.

Sharp, R. D., and R. G. Johnson, Satellite measurements of auroral particle precipitation, Earth's Particles and Fields, ed. B. M. McCormac, Reinhold Publishing Corp., New York, p. 113, 1968.

Vasyliunas, V. M., A survey of low-energy electrons in the evening sector of the magnetosphere with Ogo 1 and Ogo 3, J. Geophys. Res., 73, 2839, 1968.

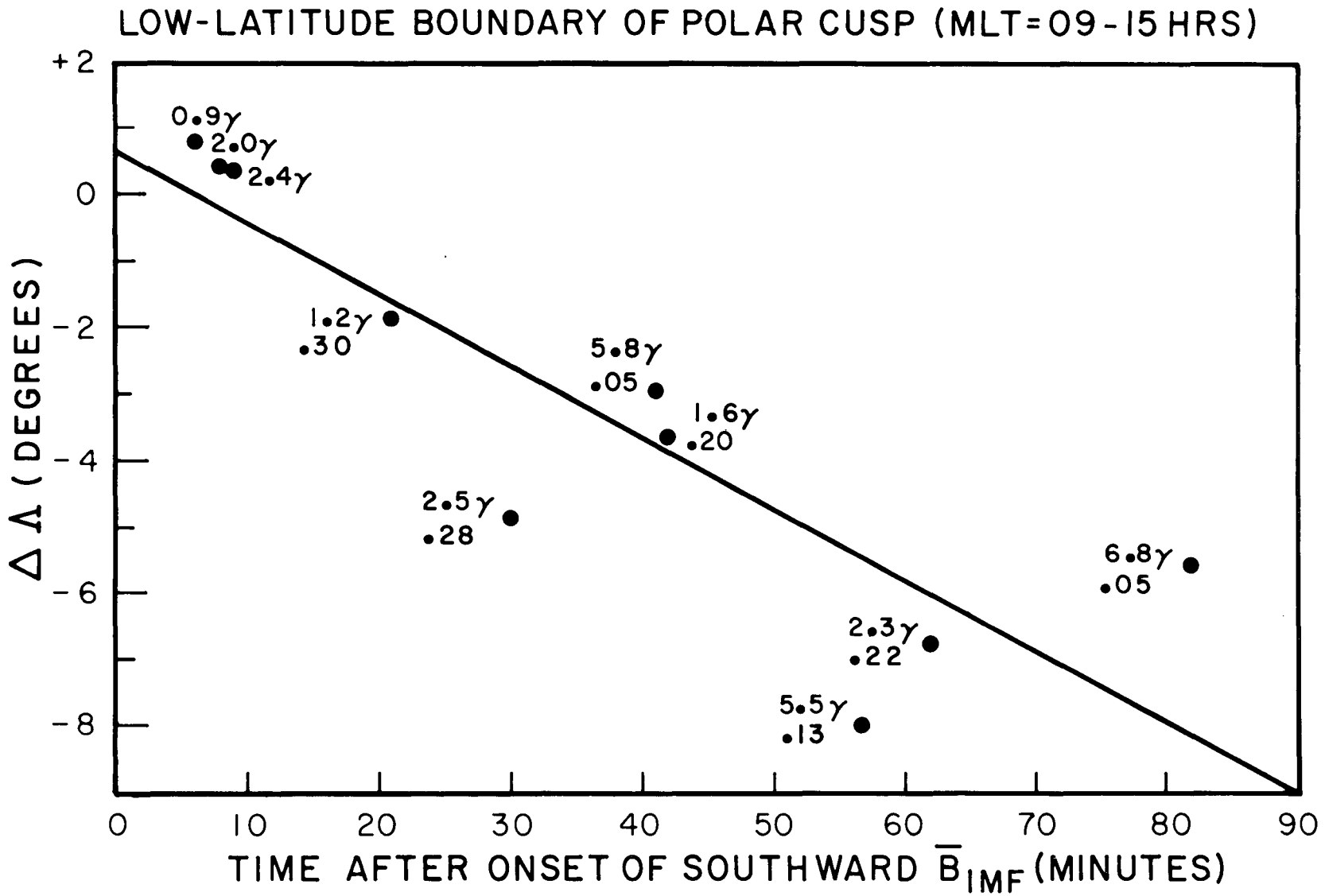
LOW-LATITUDE BOUNDARY OF POLAR CUSP (MLT=09-15 HRS)
+2
0
-2
-4
-6
-8
ΔΛ (DEGREES)
0.9γ
2.0γ
2.4γ
1.2γ
.30
5.8γ
.05
1.6γ
.20
2.5γ
.28
6.8γ
.05
2.3γ
.22
5.5γ
.13
0
10
20
30
40
50
60
70
80
90
TIME AFTER ONSET OF SOUTHWARD $\bar{B}_{IMF}$ (MINUTES)

FIGURE 1

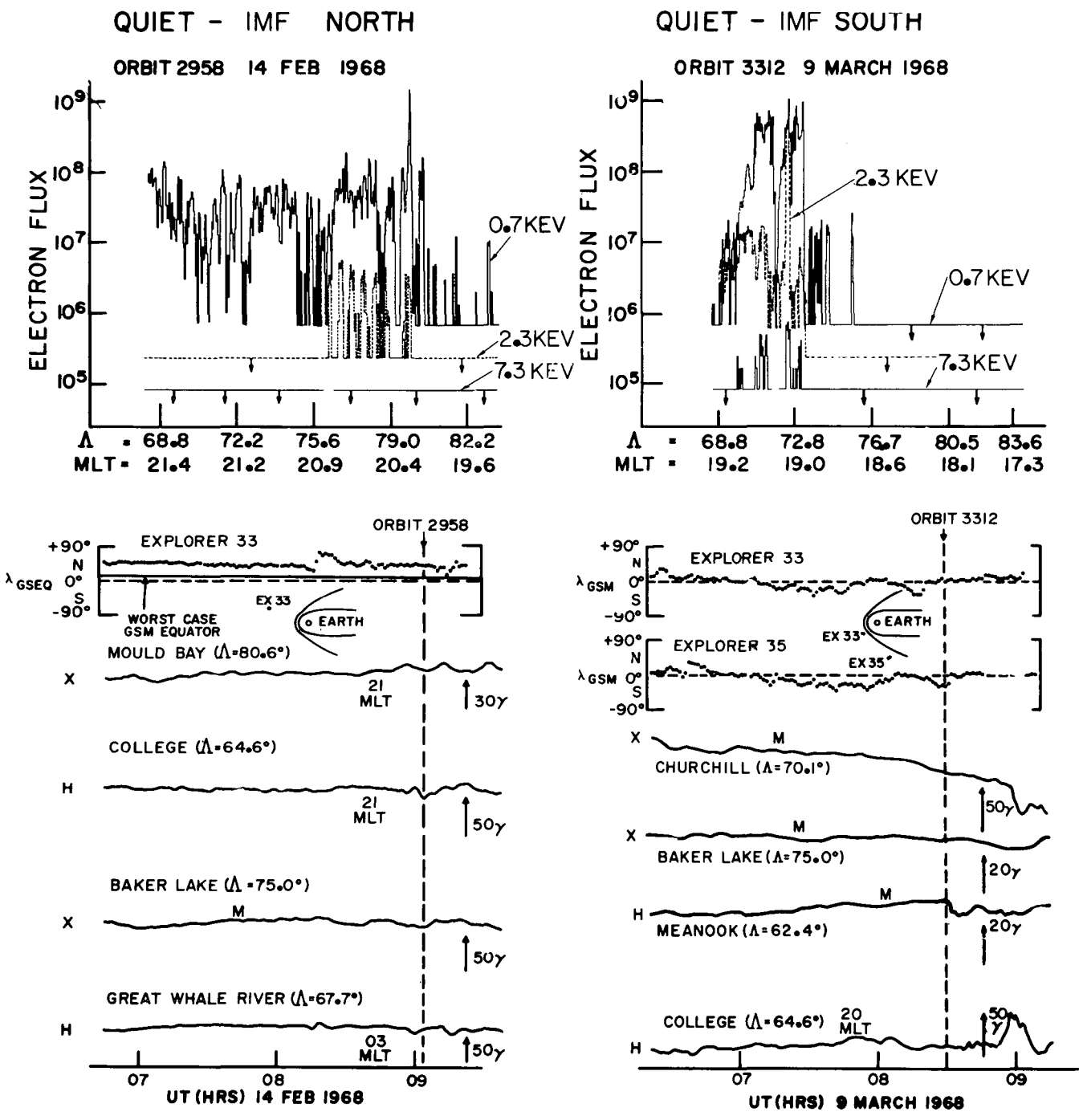
QUIET - IMF NORTH
ORBIT 2958 14 FEB 1968
ELECTRON FLUX
0.7KEV
2.3KEV
7.3 KEV
Λ = 68.8 72.2 75.6 79.0 82.2
MLT = 21.4 21.2 20.9 20.4 19.6
QUIET - IMF SOUTH
ORBIT 3312 9 MARCH 1968
2.3 KEV
0.7 KEV
7.3KEV
Λ = 68.8 72.8 76.7 80.5 83.6
MLT = 19.2 19.0 18.6 18.1 17.3
ORBIT 2958
EXPLORER 33
WORST CASE GSM EQUATOR
EX 33
EARTH
MOULD BAY (Λ=80.6°)
COLLEGE (Λ=64.6°)
BAKER LAKE (Λ=75.0°)
GREAT WHALE RIVER (Λ=67.7°)
UT (HRS) 14 FEB 1968
ORBIT 3312
EXPLORER 33
EXPLORER 35
EX 35
CHURCHILL (Λ=70.1°)
BAKER LAKE (Λ=75.0°)
MEANOOK (Λ=62.4°)
COLLEGE (Λ=64.6°)
UT (HRS) 9 MARCH 1968

FIGURE 2

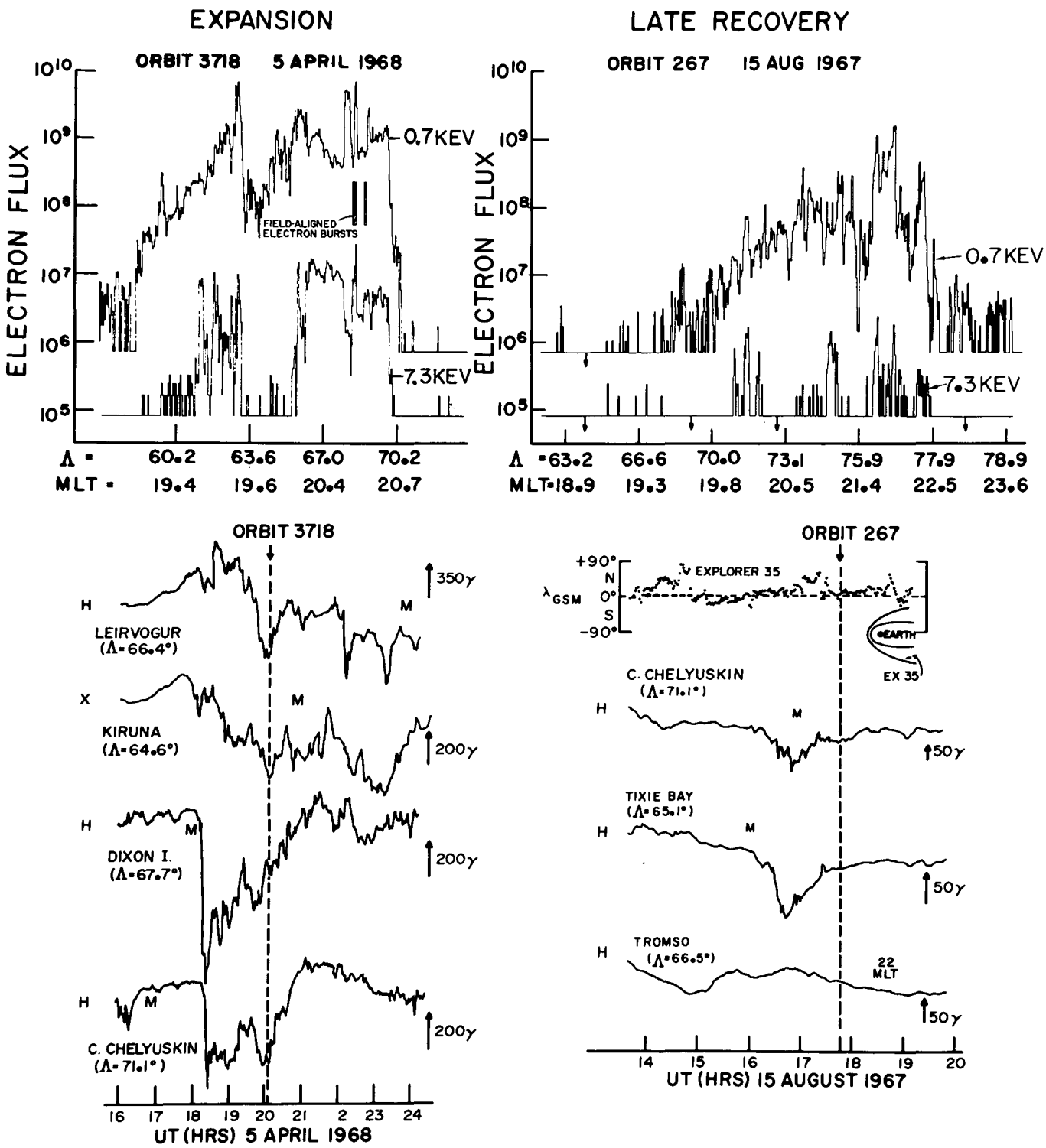
EXPANSION
ORBIT 3718 5 APRIL 1968
ELECTRON FLUX
0.7KEV
7.3KEV
FIELD-ALIGNED ELECTRON BURSTS
Λ = 60.2 63.6 67.0 70.2
MLT = 19.4 19.6 20.4 20.7
LATE RECOVERY
ORBIT 267 15 AUG 1967
0.7KEV
7.3KEV
Λ =63.2 66.6 70.0 73.1 75.9 77.9 78.9
MLT=18.9 19.3 19.8 20.5 21.4 22.5 23.6
ORBIT 3718
H
LEIRVOGUR (Λ=66.4°)
350γ
X
KIRUNA (Λ=64.6°)
200γ
DIXON I. (Λ=67.7°)
C. CHELYUSKIN (Λ=71.1°)
16 17 18 19 20 21 2 23 24
UT (HRS) 5 APRIL 1968
ORBIT 267
+90° N
λ GSM 0° S
-90°
EXPLORER 35
EARTH
EX 35
C. CHELYUSKIN (Λ=71.1°)
50γ
TIXIE BAY (Λ=65.1°)
TROMSO (Λ=66.5°)
22 MLT
14 15 16 17 18 19 20
UT (HRS) 15 AUGUST 1967

FIGURE 3

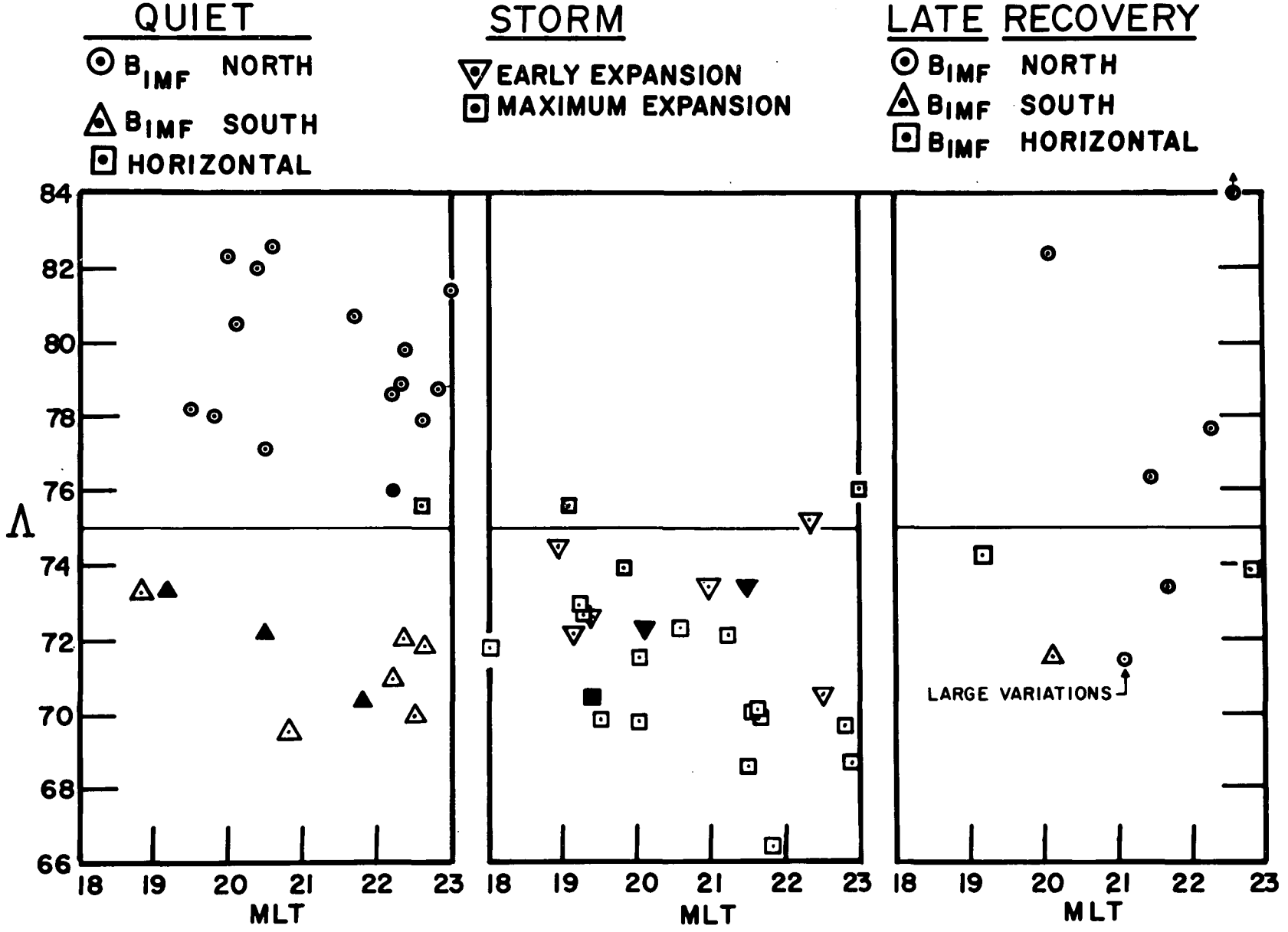
QUIET
B IMF NORTH
B IMF SOUTH
HORIZONTAL
STORM
EARLY EXPANSION
MAXIMUM EXPANSION
LATE RECOVERY
B IMF NORTH
B IMF SOUTH
B IMF HORIZONTAL
Λ
84
82
80
78
76
74
72
70
68
66
18 19 20 21 22 23
MLT
LARGE VARIATIONS

FIGURE 4

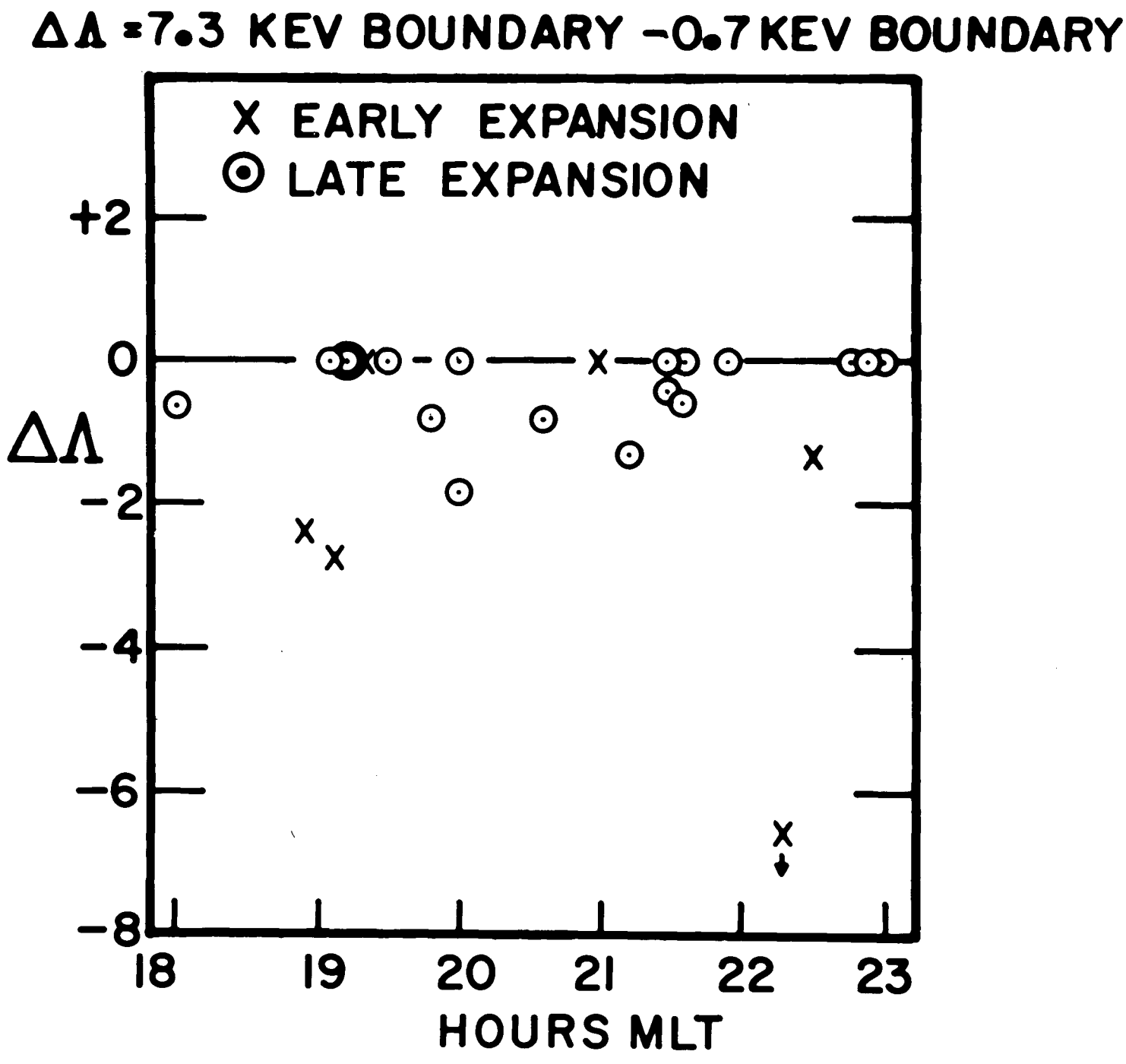
ΔΛ =7.3 KEV BOUNDARY −0.7 KEV BOUNDARY
X EARLY EXPANSION
⊙ LATE EXPANSION
+2
0
−2
−4
−6
−8
ΔΛ
18
19
20
21
22
23
HOURS MLT

FIGURE 5

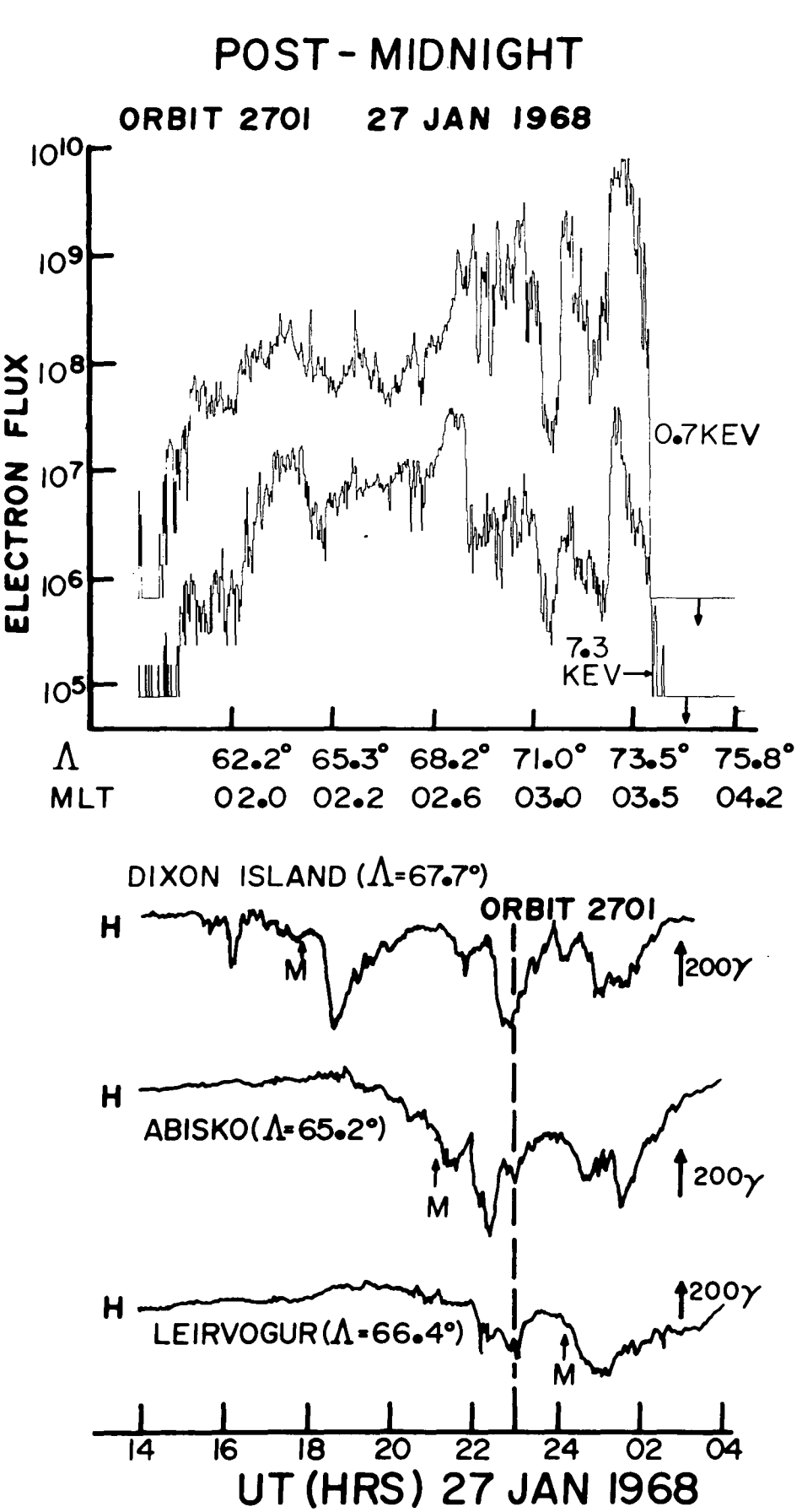
POST - MIDNIGHT
ORBIT 2701 27 JAN 1968
ELECTRON FLUX
10^10
10^9
10^8
10^7
10^6
10^5
0.7KEV
7.3
KEV
Λ
MLT
62.2° 65.3° 68.2° 71.0° 73.5° 75.8°
02.0 02.2 02.6 03.0 03.5 04.2
DIXON ISLAND (Λ=67.7°)
ORBIT 2701
H
M
200γ
H
ABISKO(Λ=65.2°)
M
200γ
H
LEIRVOGUR(Λ=66.4°)
200γ
M
14 16 18 20 22 24 02 04
UT (HRS) 27 JAN 1968

FIGURE 6

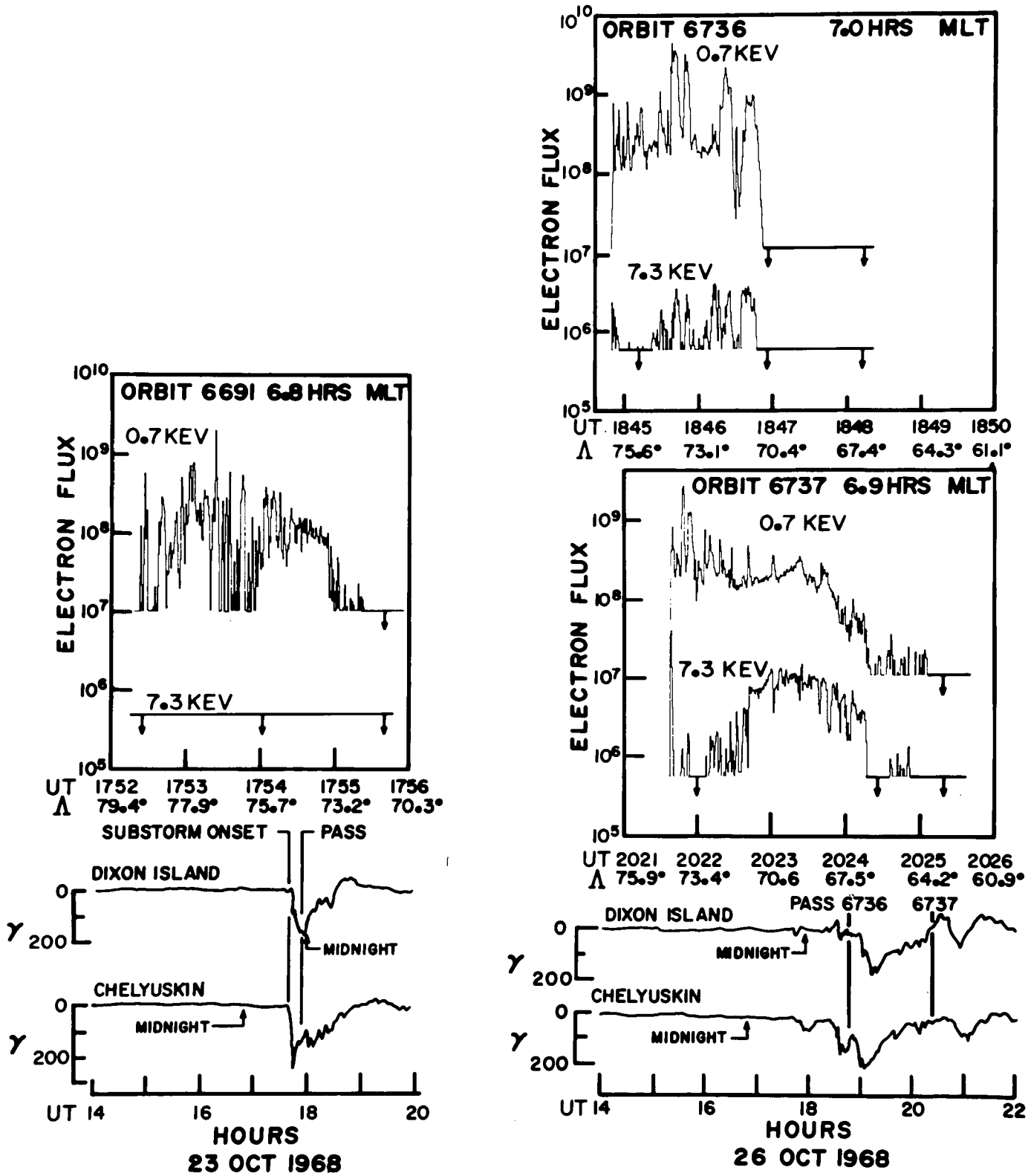
ORBIT 6736 7.0 HRS MLT
0.7 KEV
7.3 KEV
ELECTRON FLUX
UT 1845 1846 1847 1848 1849 1850
Λ 75.6° 73.1° 70.4° 67.4° 64.3° 61.1°
ORBIT 6737 6.9 HRS MLT
0.7 KEV
7.3 KEV
UT 2021 2022 2023 2024 2025 2026
Λ 75.9° 73.4° 70.6 67.5° 64.2° 60.9°
PASS 6736 6737
DIXON ISLAND
MIDNIGHT
CHELYUSKIN
UT 14 16 18 20 22
HOURS
26 OCT 1968
ORBIT 6691 6.8 HRS MLT
0.7 KEV
7.3 KEV
UT 1752 1753 1754 1755 1756
Λ 79.4° 77.9° 75.7° 73.2° 70.3°
SUBSTORM ONSET
PASS
DIXON ISLAND
MIDNIGHT
CHELYUSKIN
UT 14 16 18 20
HOURS
23 OCT 1968

FIGURE 7

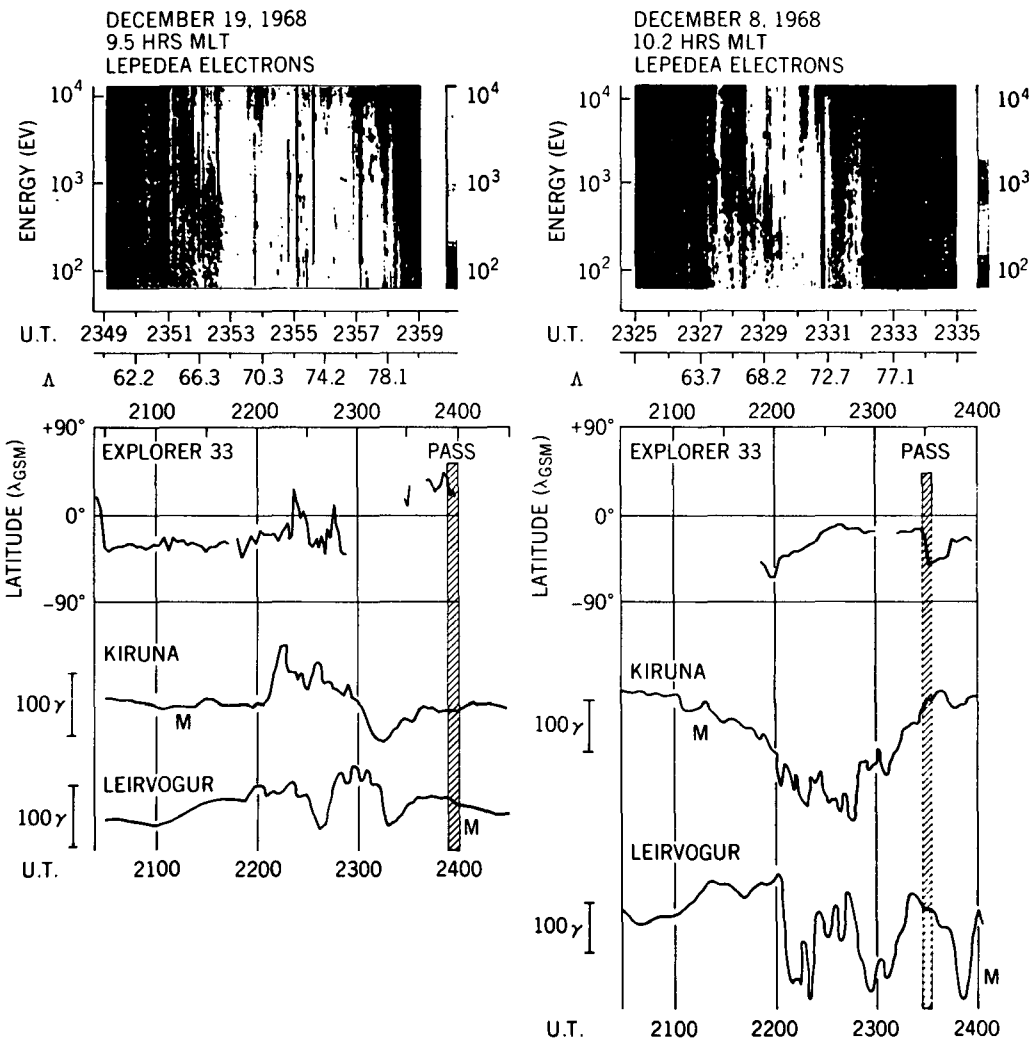
DECEMBER 19, 1968
9.5 HRS MLT
LEPEDEA ELECTRONS
ENERGY (EV)
10^4
10^3
10^2
U.T. 2349 2351 2353 2355 2357 2359
Λ 62.2 66.3 70.3 74.2 78.1
2100 2200 2300 2400
LATITUDE (λ_{GSM})
+90°
0°
-90°
EXPLORER 33
PASS
KIRUNA
100γ
M
LEIRVOGUR
100γ
M
U.T. 2100 2200 2300 2400
DECEMBER 8, 1968
10.2 HRS MLT
LEPEDEA ELECTRONS
ENERGY (EV)
10^4
10^3
10^2
U.T. 2325 2327 2329 2331 2333 2335
Λ 63.7 68.2 72.7 77.1
2100 2200 2300 2400
LATITUDE (λ_{GSM})
+90°
0°
-90°
EXPLORER 33
PASS
KIRUNA
100γ
M
LEIRVOGUR
100γ
M
U.T. 2100 2200 2300 2400

FIGURE 8

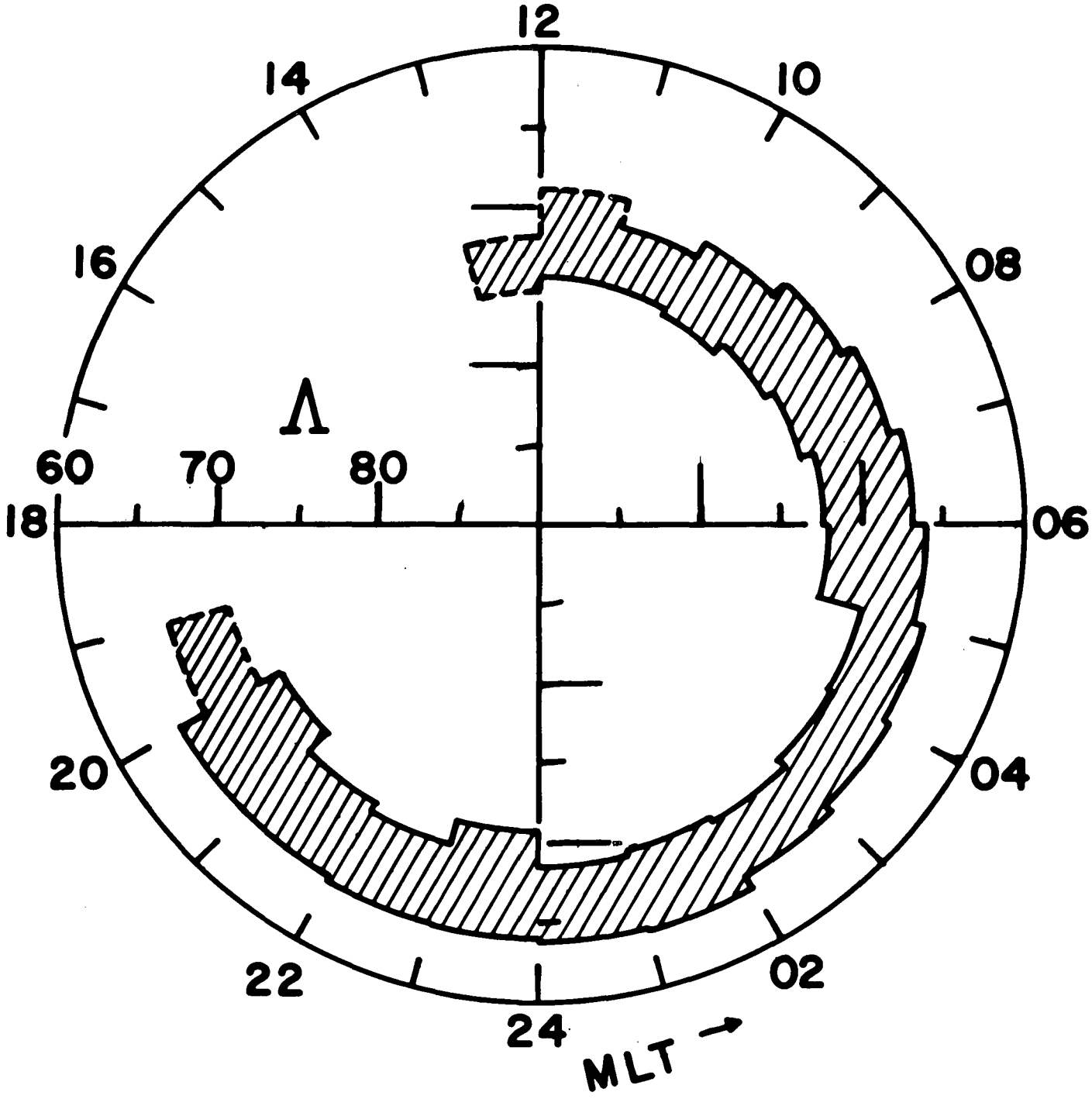

FIGURE 9

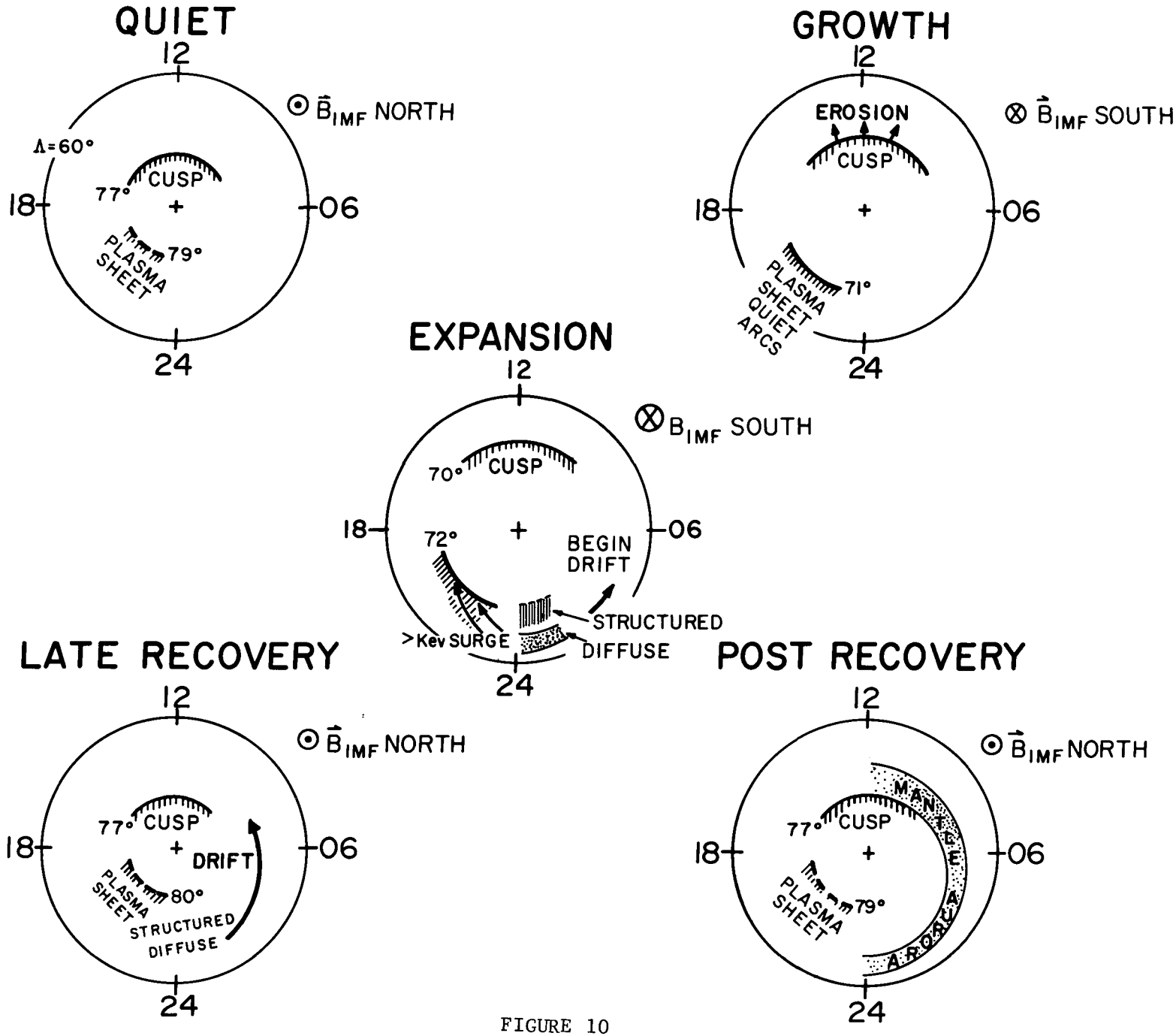
QUIET
12
$\odot \vec{B}_{IMF}$ NORTH
Λ=60°
CUSP
77°
18
06
79°
PLASMA SHEET
24
GROWTH
12
EROSION
CUSP
$\otimes \vec{B}_{IMF}$ SOUTH
18
06
PLASMA SHEET
71°
QUIET ARCS
24
EXPANSION
12
$\otimes B_{IMF}$ SOUTH
70°
CUSP
18
72°
06
BEGIN DRIFT
STRUCTURED
>Kev SURGE
DIFFUSE
24
LATE RECOVERY
12
$\odot \vec{B}_{IMF}$ NORTH
77°
CUSP
DRIFT
18
06
PLASMA SHEET
80°
STRUCTURED
DIFFUSE
24
POST RECOVERY
12
$\odot \vec{B}_{IMF}$ NORTH
MANTLE
77°
CUSP
18
06
PLASMA SHEET
79°
AURORA
24

FIGURE 10

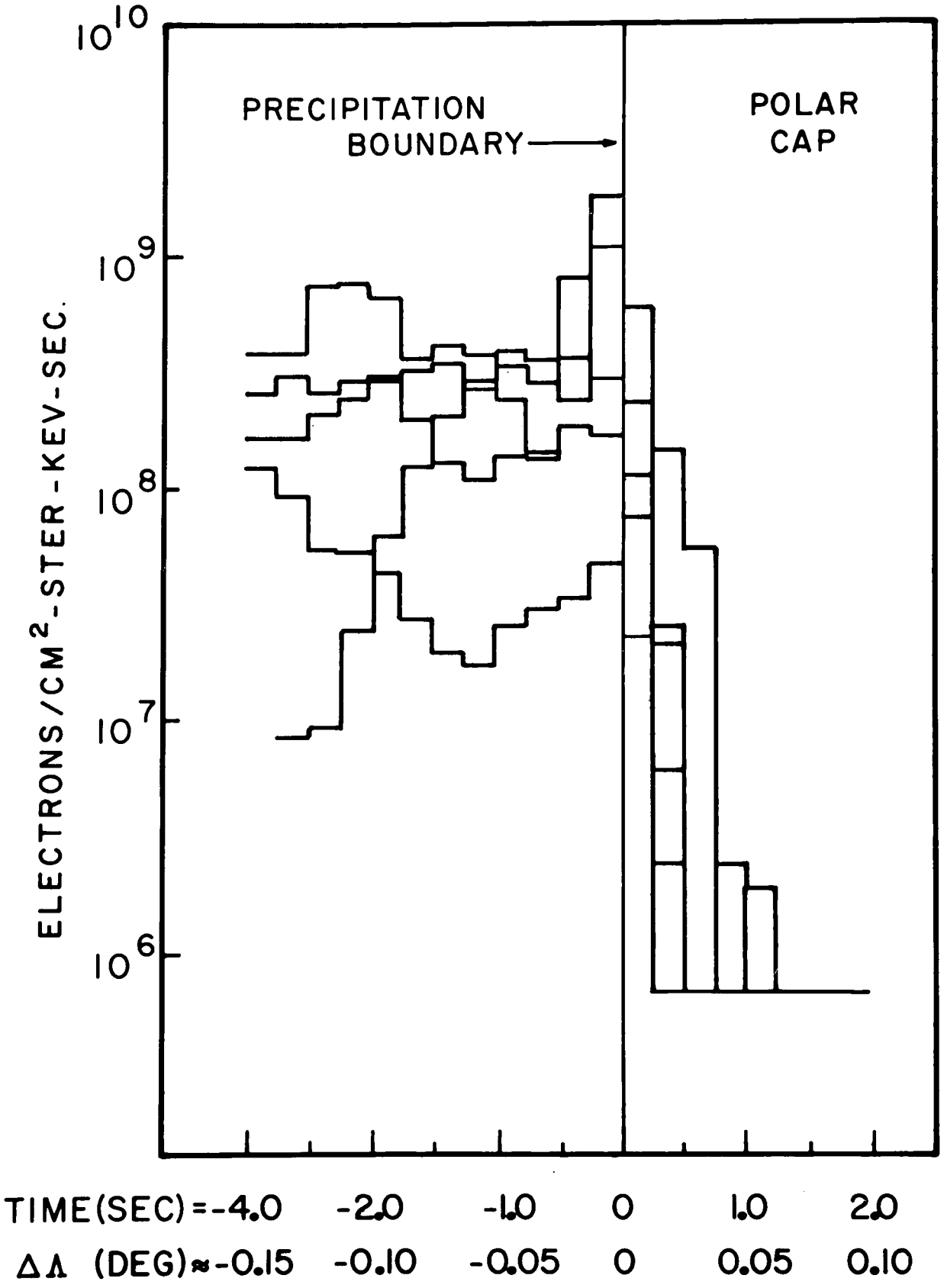
PRECIPITATION BOUNDARY
POLAR CAP
ELECTRONS/CM²-STER-KEV-SEC.
10¹⁰
10⁹
10⁸
10⁷
10⁶
TIME(SEC) = -4.0 -2.0 -1.0 0 1.0 2.0
ΔΛ (DEG) ≈ -0.15 -0.10 -0.05 0 0.05 0.10

FIGURE 11

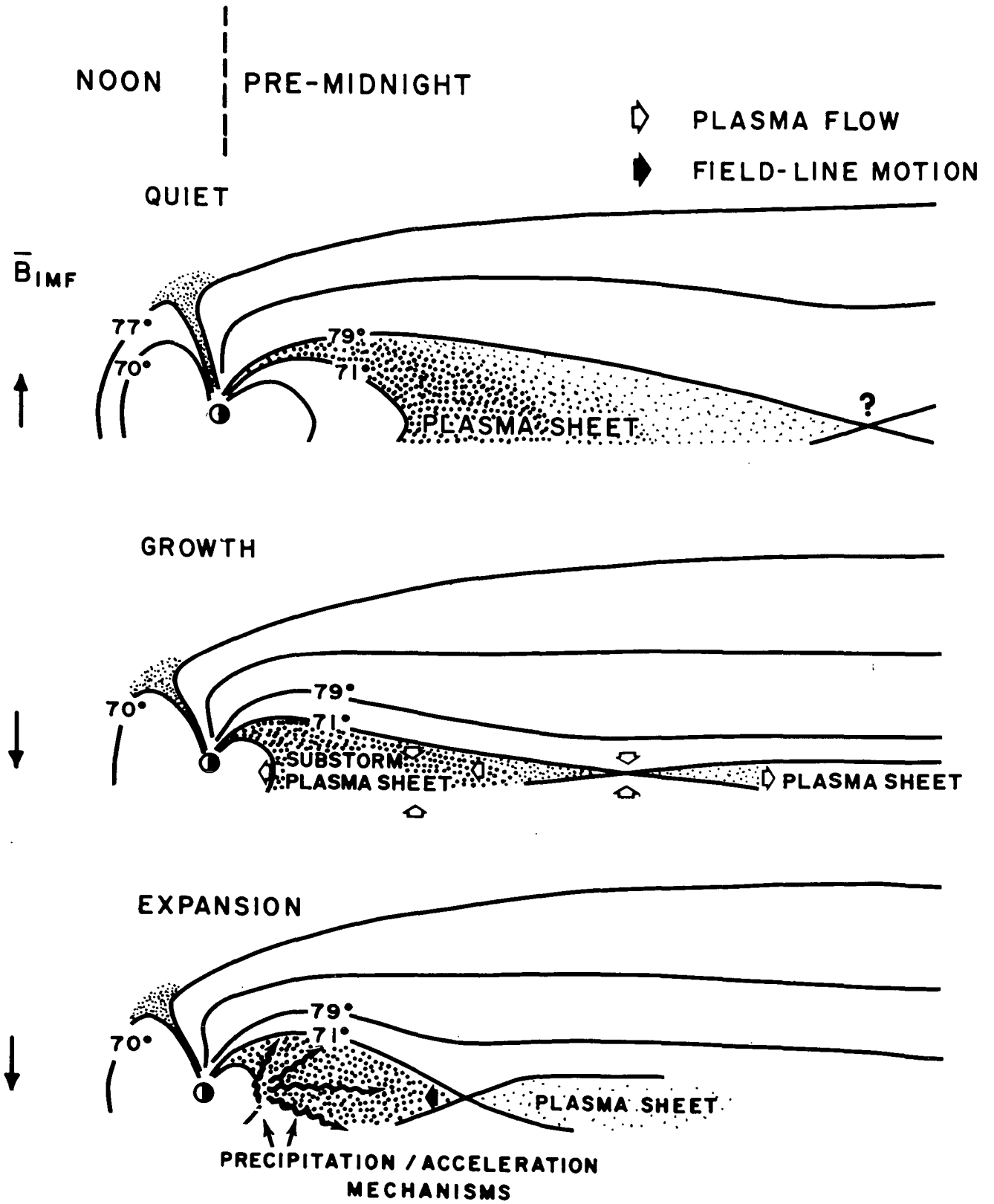

FIGURE 12

NASA–GSFC

* U.S. GOVERNMENT PRINTING OFFICE: 1972—735-962/139